Master of Science Thesis

Asymmetric capture of Dirac dark matter in the Sun

Stefan Clementz

Theoretical Particle Physics, Department of Theoretical Physics,
School of Engineering Sciences
Royal Institute of Technology, SE-106 91 Stockholm, Sweden

Stockholm, Sweden 2013

Typeset in LaTeX

Examensarbete inom ämnet teoretisk fysik för avläggande av civilingenjörsexamen inom utbildningsprogrammet Teknisk fysik.

Graduation thesis on the subject Theoretical Physics for the degree Master of Science in Engineering from the School of Engineering Physics.

TRITA-FYS 2013:46
ISSN 0280-316X
ISRN KTH/FYS/–13:46–SE

Printed in Sweden by Universitetsservice US AB, Stockholm July 2013

Abstract

There is now an overwhelming amount of evidence that support the existence of Dark Matter (DM). The most prominent candidate to explain DM is that it consist of some currently unknown particle, for example weakly interacting massive particles. Many of the proposed extensions of the Standard Model (SM) predict particles that could explain DM. An interesting feature of DM particles that interact with SM particles is that they can accumulate in astrophysical bodies. The presence of such particles in the Sun will have consequences for the solar evolution and helioseismology. If the particle has an anti particle, an asymmetry between the number of captured particles and anti particles can build up over time either because of the capture rates for DM and anti-DM being different or due to the capture being a stochastic process. In this thesis, the size of this asymmetry for both cases are investigated. The size of the asymmetry can grow to a significant size when compared to studies on solar physics using asymmetric DM. However, a study of the effects on the Sun using asymmetric capture of DM is needed to draw any conclusion.

Key words: Dark matter, Sun, Helioseismology

Sammanfattning

Det finns nu en överväldigande mängd bevis som stödjer existensen av mörk materia. Den mest framstående kandidaten för att förklara mörk materia är att den består av en okänd partikel, till exempel svagt växelverkande massiva partiklar. Många av de föreslagna utvidgningarna av standardmodellen förutspår partiklar som kan förklara mörk materia. En intressant egenskap hos mörk materia partiklar som växelverkar med partiklar i standardmodellen är att de kan ansamlas i astrofysikaliska kroppar. Närvaron av sådana partiklar i solen kommer att ha konsekvenser för solens utveckling och helioseismologi. Om partikeln har en antipartikel kan en asymmetri byggas upp över tiden, antingen för att infångningshastigheten för partiklar och antipartiklar är olika eller för att infångningsprocessen är stokastisk. I denna tes undersöks asymmetrin i båda fallen. Storleken på dessa asymmetrier kan växa till en betydande storlek vid jämförelse med studier på solfysik som använder asymmetrisk mörk materia. En studie av effekten på solen med asymmetrisk infångning av mörk materia behövs för att slutsatser ska kunna dras.

Nyckelord: Mörk materia, Solen, Helioseismologi

Preface

This thesis presents the results of my work from January 2013 to July 2013, in the Theoretical Particle Physics group at the Department of Theoretical Physics at KTH, Royal Institute of Technology. It concerns the capture of DM particles and antiparticles in the Sun.

Overview

The structure of the thesis is as follows; the thesis consists of five chapters. Ch. 1 contains a short review of the SM in which the particle content is listed and the theory of particle interactions is explained. A number of problems with the SM is listed and a short mathematical treatment of neutrino oscillation is added. In ch. 2, various experimental evidence of DM is presented along with some experiments that are attempting to detect DM directly and indirectly. Effective Lagrangians for Dirac DM-nuclei interactions and the cross sections are also looked at. In ch. 3, the capture of DM and anti-DM in the Sun by solar nuclei and already captured DM, anti-DM along with DM annihilation is discussed in detail. Ch. 4 presents the equations governing the evolution of the amount of DM and anti-DM in the Sun. The asymmetry is defined and calculated for the two cases as well. In ch. 5, the input parameters of the program is shown followed by calculations of the capture rates and self-capture rates of DM and anti-DM as well as the annihilation rate. Results regarding the amount of DM in the Sun and the size of the asymmetries are also presented. These are followed by a summary and discussion in ch. 6.

Acknowledgements

I would like to thank my supervisor Dr. Mattias Blennow for the help that I have got along the way with this thesis. Another thank you goes to Prof. Tommy Ohlsson for letting me do my diploma thesis with the Theoretical Particle Physics group. I would also like to thank all of the members of the group for providing articles for the journal club which I have enjoyed greatly. In particular, I would like to thank Bo Cao for company and many interesting, sometimes quite lively discussions and Shun Zhou for joining us during our lunches. I would also like to

thank my family for everything that they have done for me during my time spent at KTH.

Contents

Chapter 1

Introduction

The idea of elementary particles dates back to ancient Greece several centuries BC. The meaning of the word atom is to be indivisible. The concept of physical atoms was first used to explain why elements combine to form compounds in small number ratios. In 1897, Joseph J. Thompson discovered the electron [1]. He drew the conclusion that the electron was a component of the, no longer indivisible, atoms. Later, Ernest Rutherford concluded from an experiment that elements have a massive, positively charged nucleus. In 1918, he discovered the proton as the nucleus of hydrogen. He also predicted the existence of the neutron by the mass of different isotopes changing in multiples of a certain number. The neutron was found by James Chadwick in 1932 [2]. With the development of particle accelerators and detectors, a huge number of different particles were found. So many in fact, that Murray Gell-Mann and George Zweig in 1964 independently proposed the quark model, in which all known hadrons were composed of three quarks, the up, down and strange quark [3, 4]. Deep inelastic scattering experiments of the proton showed that it was, in fact built up by point-like objects called partons, a collective name for quarks, anti quarks and gluons. The charm quark was proposed because it allowed for a better description of the weak interaction. Later the top and bottom quarks were proposed to explain observations of CP-violation. All of the particles of the SM have been found in experiments, with the Higgs boson being found in 2012, some 40 years after it was predicted. While the SM, as it is, has produced astonishing predictions of the particles and their attributes, it does have some problems.

1.1 The standard model of particle physics

The SM is the theory that describe the fundamental particles and their interactions via the electromagnetic, weak and strong nuclear forces. The strong force model, or Quantum Chromodynamics as it is called, is a non-Abelian gauge theory with gauge group $SU(3)_c$. The electroweak interaction model is also a non-Abelian gauge

theory but with gauge group $SU(2)_L \otimes U(1)_Y$. The SM is thus a non-Abelian gauge group theory with gauge group $SU(3)_c \otimes SU(2)_L \otimes U(1)_Y$.

1.1.1 Particles

The fundamental particles of the SM are divided into two categories that are separated by the spin of the particles. The two categories are the fermions which have a spin of 1/2 while all bosons have a spin of 1 (except for the Higgs boson which is spinless).

The fermions

The fermionic sector contain three generations of quarks and three generations of leptons. The leptons are:

$$\begin{pmatrix} \nu_e \\ e \end{pmatrix}, \begin{pmatrix} \nu_\mu \\ \mu \end{pmatrix}, \begin{pmatrix} \nu_\tau \\ \tau \end{pmatrix}. \tag{1.1}$$

The leptons are not charged under the color group, however, the e, μ and τ have electric charge -1 while the ν_e, ν_μ and ν_τ are neutral. The quarks are paired in a similar way:

$$\begin{pmatrix} u \\ d \end{pmatrix}, \begin{pmatrix} c \\ s \end{pmatrix}, \begin{pmatrix} t \\ b \end{pmatrix}. \tag{1.2}$$

The u, c and t quarks have electric charge $+2/3$ while the d, s and b quarks have electric charge $-1/3$. The quarks also carry a color charge.

Each generation of quarks is heavier than the previous one with the u and d quarks being the lightest. The same holds true for the charged leptons with e being the lightest. The masses of the neutrinos are not yet known.

Any fermion field can be decomposed into a left-handed and a right-handed part using the projection operators

$$\psi = P_L\psi + P_R\psi = \psi_L + \psi_R, \tag{1.3}$$

where the projection operators are defined as

$$P_L = \frac{1-\gamma^5}{2} \quad , \quad P_R = \frac{1+\gamma^5}{2} \tag{1.4}$$

with $\gamma^5 = i\gamma^0\gamma^1\gamma^2\gamma^3$, where γ^μ are the Dirac matrices.

In the SM, the left- and right-handed components couple differently to gauge bosons. Right handed fields are singlets under the $SU(2)_L$ group while left handed

fields are assigned to $SU(2)_L$ doublets. The particle content for generation $i = 1, 2, 3$ can be summed up as:

$$E_L^i = \begin{pmatrix} \nu_L^i \\ e_L^i \end{pmatrix} \ , \ Q_L^i = \begin{pmatrix} u_L^i \\ d_L^i \end{pmatrix} \ , \ e_R^i \ , \ u_R^i \ , \ d_R^i. \tag{1.5}$$

Right-handed neutrinos have no charge under any of the SM gauge groups. They are thus not introduced in the SM since experimental verification of their existence would be impossible.

The gauge bosons

The $SU(3)_c$ gauge group introduces eight massless gluons that mediate the color force between color charged particles. Apart from the gluons themselves, only quarks carry color. Thus, the only strongly interacting particles in the SM are the gluons and the quarks.

Spontaneous symmetry breaking of the electroweak theory occur through the Higgs mechanism [5–7]. The electroweak symmetry breaking (EWSB) produces three massive and one massless gauge boson along with the Higgs boson. These gauge bosons are the massive weak force carriers W^+, W^- and the Z^0, and the massless gauge boson is the electromagnetic force carrier γ, the photon.

1.1.2 Particle interactions

In the framework of the SM, interactions via force carriers come about by requiring gauge invariance of the Lagrangian under the group transformations. For example, consider the Lagrangian of a free fermion field

$$\mathcal{L}_{\text{free}} = \bar{\psi}(i\partial\!\!\!/ - m)\psi. \tag{1.6}$$

We want to construct a Lagrangian that is invariant under a local $U(1)$ transformation, that is

$$\psi(x) \to e^{i\alpha(x)}\psi(x). \tag{1.7}$$

Due to the derivative term, the Lagrangian in eq. (1.6) is obviously not invariant under the transformation. If we introduce the covariant derivative

$$D_\mu = \partial_\mu + igA_\mu, \tag{1.8}$$

where g is the coupling constant and A_μ is the connection, which transforms as

$$A_\mu(x) \to A_\mu(x) - \frac{1}{g}\partial_\mu\alpha(x), \tag{1.9}$$

then

$$D_\mu\psi(x) \to [\partial_\mu + ig(A_\mu - \frac{1}{g}\partial_\mu\alpha(x))]e^{i\alpha(x)}\psi(x) = e^{i\alpha(x)}D_\mu\psi(x). \tag{1.10}$$

The field strength tensor of $A_\mu(x)$, which is defined as:

$$F_{\mu\nu} = \partial_\mu A_\nu - \partial_\nu A_\mu \tag{1.11}$$

is also invariant under the transformation given in eq. (1.9). We can now write down a Lagrangian that is invariant under a local $U(1)$ transformation

$$\mathcal{L} = \mathcal{L}_{\text{free}} - \frac{1}{4}(F^{\mu\nu})^2 - g\bar{\psi}\gamma^\mu\psi A_\mu. \tag{1.12}$$

The last piece in the equation above explains the interaction of the fermion fields with the vector field A_μ. In fact, if we change g to the electric charge e and call the vector field A_μ a photon, we find that we have just written down the Lagrangian of Quantum Electrodynamics. The same procedures apply to the other gauge groups of the SM. For non-Abelian gauge groups, such as the $SU(2)$ and $SU(3)$ gauge groups, $F_{\mu\nu}{\rightarrow}F^a_{\mu\nu}$ which has an additional term $gf^{abc}A^b_\mu A^c_\nu$ where f^{abc} is the structure constant.

The electroweak $SU(2)_L{\otimes}U(1)_Y$ covariant derivative is

$$D_\mu = \partial_\mu - igW^a_\mu T^a - ig'B_\mu Y \tag{1.13}$$

where $a = 1, 2, 3$ and Y is the hypercharge. After spontaneous symmetry breaking, the four vector fields $(W^1, W^2, W^3)_\mu$ and B_μ mix to form the weak and electromagnetic force carriers. T^a is related to the three Pauli matrices.

The covariant derivative of the color group $SU(3)_c$ is

$$D_\mu = \partial_\mu - igG^a_\mu T^a \tag{1.14}$$

with $a = 1, ..., 8$. The eight vector fields G^a_μ are the gluons and T^a are related to the Gell-Mann matrices.

1.1.3 Electroweak Symmetry Breaking and the Higgs boson

As mentioned before, the EWSB occurs through the Higgs mechanism. It is also how the other elementary particles of the SM receive their masses. Introduce a $SU(2)_L$ doublet field ϕ with charge 1/2 under the $U(1)_Y$ group. Let ϕ acquire a vacuum expectation value (VEV)

$$\langle\phi\rangle = \frac{1}{\sqrt{2}}\begin{pmatrix} 0 \\ v \end{pmatrix}. \tag{1.15}$$

The covariant derivative of ϕ is given by eq. (1.13). The mass terms then arise from the square of the $D_\mu\phi$ term, using $T^a = \frac{\sigma^a}{2}$ and the VEV of the Higgs field:

$$\mathcal{L}_{\text{mass}} = \frac{v^2}{8}[g^2(W^1_\mu)^2 + g^2(W^2_\mu)^2 + (gW^3_\mu - g'B_\mu)^2]. \tag{1.16}$$

We can now define the four vector fields, and identify the weak and electromagnetic vector bosons

$$\begin{aligned} W_\mu^\pm &= \frac{1}{\sqrt{2}}(W_\mu^1 \mp W_\mu^2) \text{ with mass } M_W = \frac{gv}{2} \\ Z_\mu^0 &= \frac{1}{\sqrt{g^2+g'^2}}(gW_\mu^3 - g'B_\mu) \text{ with mass } M_Z = \sqrt{g^2+g'^2}\frac{v}{2} \\ A_\mu &= \frac{1}{\sqrt{g^2+g'^2}}(g'W_\mu^3 + gB_\mu) \text{ with mass } M_A = 0 \end{aligned} \tag{1.17}$$

The field ϕ can be defined in terms of in terms of a real field $h'(x)$ with $\langle h'(x)\rangle = v$ and a general $SU(2)$ transformation $U(x)$

$$\phi(x) = \frac{1}{\sqrt{2}}U(x)\begin{pmatrix} 0 \\ h'(x) \end{pmatrix}. \tag{1.18}$$

One can always choose a gauge such that ϕ is unchanged by $U(x)$. The field ϕ can then be expanded around its VEV as $h'(x)\to v + h(x)$. The covariant derivative then give rise to the vector boson masses and interactions with a new real scalar particle $h(x)$ which is called the Higgs boson. The Higgs boson was found in 2012 by the ATLAS and CMS detectors which analyze collisions in the Large Hadron Collider at CERN [8, 9].

It is also possible to write down gauge invariant couplings between the left- and right-handed parts of fermion fields and the Higgs boson. The coupling for leptons would be

$$\Delta\mathcal{L} = -\lambda_i \bar{E}_L^i \phi l_R^i + h.c., \tag{1.19}$$

where i denotes the generation. When the Higgs field acquire its VEV, we get

$$\Delta\mathcal{L} = -\lambda_i \frac{v}{\sqrt{2}}\bar{l}_L^i l_R^i + h.c., \tag{1.20}$$

which are mass terms for the leptons. For the quarks, the mass terms are generated by

$$\Delta\mathcal{L} = -\lambda_{d,i}\bar{Q}_L^i \phi d_R^i - \lambda_{u,i}\epsilon^{ab}\bar{Q}_{La}^i \phi_b d_R^i + h.c. \tag{1.21}$$

Without the right-handed neutrino, there is no similar way to write down a neutrino mass term which lead to massless SM neutrinos.

1.2 Problems of the Standard Model

Even though the SM has made extremely accurate predictions of the behaviour of particles, it is not perfect. The SM has a number of issues that need to be solved.

A major issue is the incompatibility with the general theory of relativity which very successfully describes gravity. Naturally, one would like to form a single theory which explains all four forces that we know of.

There is no explanation for DM and Dark Energy. DM is necessary to explain for example the gravitational curves of galaxies and the velocity dispersion of galaxies in galaxy clusters. The only candidate for particle DM in the SM is the neutrino which, because of its mass and abundance, can only form a small fraction of the DM. Dark energy refers to the phenomenon that the universe not only expand, but that it does so at an accelerating pace. While the cosmological constant Λ of the Einstein field equations successfully describes the accelerating expansion of the universe, the reason for its existence and why it has the value that it has is unknown.

Another problem is the asymmetry of matter and anti-matter. The SM predicts that the big bang should have produced essentially equal amounts of matter and anti-matter. We owe our existence to an asymmetry between the number of matter and anti-matter particles in the early universe. For every billion of anti-matter particles, there was a billion and one particles. The anti-matter annihilated and left was a tiny amount of matter. The famous Sakharov conditions is a set of three conditions a baryon-generating interaction must satisfy. These are baryon number violation, C and CP violation, and interactions out of thermal equilibrium. The electroweak baryogenesis seem to be a too small contribution to account for the entire asymmetry.

The most immediate issue is the neutrino masses. The neutrinos can spontaneously change flavor, a phenomenon called neutrino oscillation. It has been experimentally verified by many experiments [10–14] and it is the solution to the solar neutrino problem where about only a third of the expected neutrino flux was measured in charged current interactions.

The issues explained above are the more famous that need to be solved. There are a number of other oddities that physicists hope to explain with beyond SM theories such as supersymmetry and string theory.

1.2.1 Neutrino oscillations

Due to the absence of right-handed neutrinos in the SM, mass acquisition by interacting with the Higgs field is not possible. However, the oscillation of neutrinos indicate that they do have a mass. Consider the case of three neutrino species ν_α where $\alpha = e, \mu, \tau$ and relate them to three neutrino mass eigenstates by the Pontecorvo-Maki-Nakagawa-Sakata (PMNS) matrix [15], which is usually written as:

$$U = \begin{pmatrix} c_{12}c_{13} & s_{12}c_{13} & s_{13}e^{-i\delta} \\ -s_{12}c_{23} - c_{12}s_{23}s_{13}e^{i\delta} & c_{12}c_{23} - s_{12}s_{23}s_{13}e^{i\delta} & s_{23}c_{13} \\ s_{12}s_{23} - c_{12}c_{23}s_{13}e^{i\delta} & -c_{12}s_{23} - s_{12}c_{23}s_{13}e^{i\delta} & c_{23}c_{13} \end{pmatrix}, \quad (1.22)$$

where $s_{ij} = \sin\theta_{ij}$, $c_{ij} = \cos\theta_{ij}$, θ_{ij} are mixing angles and δ is the CP-violating phase. In the case of neutrinos being majorana particles, one must multiply U by a matrix $\mathrm{diag}(e^{i\alpha_1/2}, e^{i\alpha_2/2}, 1)$, where α_i are majorana phases. With the PMNS matrix, a neutrino of flavor α is, in terms of its mass eigenstates $|\nu_i\rangle$:

$$|\nu_\alpha\rangle = \sum_{i=1}^{3} U^*_{\alpha i} |\nu_i\rangle . \tag{1.23}$$

To each mass eigenstate i is associated the definite mass m_i. The neutrino satisfy the Dirac equation and $|\nu_i\rangle$ will have have plane wave solutions

$$|\nu_i(\vec{x}, t)\rangle = e^{-i(Et - \vec{p_i}\vec{x})} |\nu_i(0)\rangle . \tag{1.24}$$

Here $\vec{p_i}$ and $\vec{x}$ are parallel, $t{\approx}|x|$ and the energy is given by $E = \sqrt{p_i^2 + m_i^2}$. Assuming $m_i{\ll}|p_i|{\approx}E$, then we can expand the energy in terms of momenta

$$E = \sqrt{m_i^2 + p_i^2} \approx p_i + m_i^2/2p_i. \tag{1.25}$$

The time evolution of state i is then obtained by using $p_i{\approx}E$ and plugging the above into eq. (1.24)

$$|\nu_i(t)\rangle = e^{-i\frac{m_i^2}{2E}t} |\nu_i(0)\rangle . \tag{1.26}$$

The probability of detecting a neutrino of species β at time t is given as

$$\begin{aligned} P_{\alpha\to\beta} &= \left| \langle \nu_\beta | \nu_\alpha(t) \rangle \right|^2 \\ &= \left| \sum_{i=1}^{3} U_{\beta i} U^*_{\alpha i} e^{-i\frac{m_i^2}{2E}t} \right|^2 \\ &= \sum_{i=1}^{3}\sum_{j=1}^{3} U_{\beta i} U^*_{\alpha i} U^*_{\beta j} U_{\alpha j} e^{-i\frac{m_{ij}^2}{2E}t} \end{aligned} \tag{1.27}$$

where $m_{ij}^2 = m_i^2 - m_j^2$. Thus, massless neutrinos do not oscillate in vacuum. One effect of the accumulation of DM in the Sun is that annihilation of it will produce a, hopefully, detectable flux of neutrinos. This indirect detection of DM and the reconstruction of its properties will be discussed in the next chapter.

Chapter 2

Dark Matter

The phrase "dark matter" was first coined in the 1930s by Fritz Zwicky when he concluded that the Coma cluster needed much more mass than was visible for the high velocity galaxies to be gravitationally bound to it [16]. Soon after, it was noted that the high orbital velocities of stars in the outer regions of galaxies required them to carry much more mass than what one observed [17]. The problem was swept under the rug as observational errors for a few decades until the same conclusions were drawn from many new observations from the 1970s and forward. DM can also be mapped out through gravitational lensing of galaxy clusters. In particular colliding galaxy clusters show areas in the cluster with very little luminous matter but very high mass densities, examples being the Bullet cluster [18] and the Abell 520 cluster [19]. Many experiments have made measurements of the cosmic microwave background (CMB). The three most prominent of these are COBE, WMAP and Planck [20–22]. The cosmological standard model, ΛCDM, combined with these measurements give a prediction of how much DM there is in the Universe. All of these methods assume that the theory of general relativity is correct, which naturally spawned a few alternative theories of gravity such as modified newtonian gravity (MOND) and Nonsymmetric Gravitational Theory [23, 24]. According to [18], even taking MOND into account, DM is necessary to explain the Bullet cluster observation.

2.1 Particle dark matter

The simplest and most popular theory of DM is that it is a particle. DM particles must be electrically neutral and have a very small interaction with ordinary matter. They must also be stable or have a lifetime comparable to or longer than that of the universe for a significant fraction to still exist. In the ΛCDM model, DM was cold - non-relativistic already at the time of freeze-out. This is necessary for the structure formation in the early universe as cold DM enhances mass anisotropies

while hot DM does not. The only DM candidate in the SM is the neutrino, which is disqualified on the basis that it is not massive/abundant enough and would constitute hot DM. Many extensions of the SM which are proposed to solve other problems of the SM predict the existence of particles which fit the criteria for particle DM. The neutralino from the super symmetry (SUSY) extension has been very thoroughly studied [25]. Since searches for SUSY provide no evidence, the other DM candidates have gotten more attention. These include the axion, Kaluza-Klein DM and sterile neutrinos (many more can be found in ref. [26]). There is currently a wealth of experiments attempting to detect DM, both directly and indirectly.

2.1.1 Direct detection of dark matter

As DM scatters with a nucleus, some momenta is transferred to the nucleus it scattered off. The momenta transferred is related to the mass of the DM while the number of scattering events relate to the interaction cross section. The DAMA/LIBRA experiment have claimed a strong annual modulation signal [27] and is backed by CRESST, CoGeNT and CDMS which also claim to see an excess of events [28–30]. The favoured DM cross sections and masses for these experimental results do not agree. Results of the XENON100 experiment rule them out completely while EIDELWEISS, PICASSO and other experiments rule out most of the parameter space for these low-mass DM particles [31–33]. The current spin independent low mass DM-nucleon cross section limits are presented in figure 2.1. For DM masses between $50 - 1000$ GeV, most experiments place the upper limit on the spin independent cross section below 10^{-43} cm^2. No signs of DM have been seen in direct detection experiments at larger DM masses. The limits on spin dependent DM-proton cross sections are shown in figure 2.2. These are generally much weaker which has to do with the cross section of DM-nuclei scattering as well as the element isotopes that are used in experiments. The upper limits for DM-proton and DM-neutron cross sections for DM masses between $10 - 10^4$ GeV are below 10^{-37} cm^2 [34].

2.1.2 Indirect detection of dark matter

DM particles are thought to annihilate or decay into SM particles. By assuming specific decay channels, the flux at various energies can be calculated and measured by experiments. Of experimental interest are mainly the detection of positrons, antiprotons, high energy photons and neutrinos. By using the experimental data and comparing with the predictions of the flux, one may be able to reconstruct the DM properties.

The Fermi-LAT, PAMELA and AMS-02 [35–37] experiments measure an increase in the high-energy positron fraction that is inconsistent with the value expected from astrophysics. DM annihilating into electron-positron pairs would necessarily increase the fraction of positrons. However, it is possible that this excess

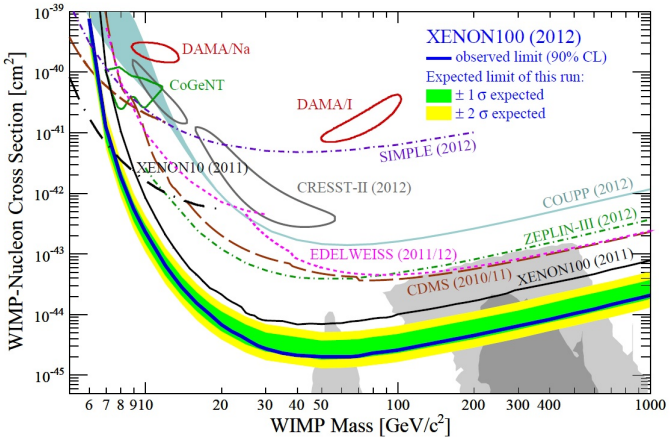

Figure 2.1. The current upper limits for the DM-nucleon spin independent cross sections. The lines correspond to upper limits on the spin independent cross sections while encircled areas are positive signals from experiments. The figure is reproduced with permission from [31].

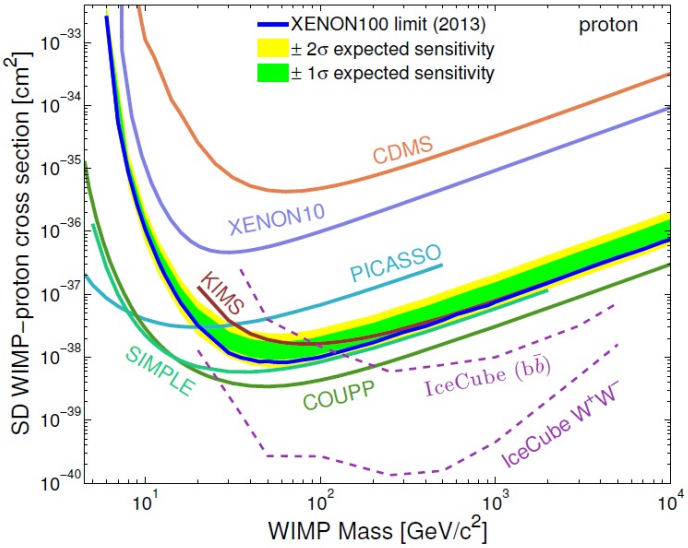

Figure 2.2. The current upper limits for the DM-proton spin dependent cross sections. Lines correspond to upper limits. The figure is reproduced with permission from [34].

of positrons can be attributed to pulsars [38] or other places where cosmic rays are accelerated, such as supernovae [39].

Experiments such as H.E.S.S., MAGIC and the Fermi gamma-ray telescope look for gamma rays from annihilation of DM, for instance in dwarf galaxies and the galactic center [40–44]. The most interesting gamma ray observations are those of monochromatic photons which show up as a sharp peak in the energy spectrum. Examples of monochromatic photon producing annihilations are $\bar{\chi}\chi \to \gamma\gamma$, $\bar{\chi}\chi \to Z^0\gamma$ and $\bar{\chi}\chi \to \phi\gamma$. A continuous spectrum can also be created by DM annihilating into unstable SM particles which in turn decay into photons.

If neutrinos are part of the final products after DM annihilation, neutrino telescopes can be used in the hunt for DM. The energy spectrum of neutrinos could look like the one for photons. If DM could annihilate directly into neutrino-anti neutrino pairs, these would be mono-energetic and show up as a peak in the energy spectrum. A continuous spectrum could also be created by decay of unstable SM particles the DM decayed into. The neutrino telescopes ANTARES, IceCube and Super-Kamiokande are currently conducting searches for DM [45–47]. Moreover, one can assume specific annihilation channels in which neutrinos are produced. The DM properties can then be reconstructed by measuring the flux of these neutrinos [48–50].

2.1.3 Effects of particle dark matter in the Sun

Early solar models predicted a neutrino flux on the Earth that did not match the one detected in experiments. Among the proposed solutions to this solar neutrino problem was particle DM [51]. Here, DM particles are introduced to help transport heat from the solar interior into outer regions, effectively lowering the temperature in the core. Since the neutrino production is heavily dependent on temperature and the neutrino flux decrease if temperature decrease. The Sudbury Neutrino Observatory measurement showed that while the expected flux of electron neutrinos was much lower, the flux of all active neutrino species matched the one expected from the solar model [11] giving definite proof of neutrino oscillations. The theoretical predictions of the standard solar model and observations were excellent until observations of photospheric abundances of heavier elements required a lowering of these abundance [52]. The match between standard solar model and observations no longer hold but now we face the solar composition problem [53]. Newer solar composition models cannot explain the observations [54] which have prompted a revisit to DM in the Sun using asymmetric DM [55–57]. In [55], it is concluded that a 5 GeV particle would restore the agreement between the standard solar model and helioseismology when the number of DM particles relative to the number of solar nuclei after 4.5 billion years is about 10^{-12}. In [56], DM with a mass of less than 10 GeV is ruled out due to constraints on the core sound speed. A fourth study focusing on the gravitational effects of captured DM on the Sun [58] limit the total mass of DM inside the Sun to about $0.02 - 0.05$ solar masses.

Annihilating or decaying DM also produce neutrinos and also that way affect the neutrino flux in a predictable way. Since neutrinos interact so weakly with ordinary matter, DM annihilation in the Sun may produce a neutrino flux that is detectable in the neutrino telescopes.

2.2 Effective Dirac dark matter theories

When introducing particle DM, it is usually accompanied by other particles through which it interact. If the Lagrangian describing these interactions is unknown, one can assume that the DM particles interact with SM fermions through heavier scalar, vector and tensor particles and integrate these out by using the equations of motion (this is done for example in ref. [59]). For Dirac DM, the most general effective lagrangian can be written

$$\mathcal{L}_{\text{eff}} = \sum_n \frac{\mathcal{O}^n}{\Lambda^{n-4}}, \tag{2.1}$$

where $\mathcal{O}^n$ is a field operator of dimension $n = 5, 6, \ldots$ and Λ is "the scale of new physics", essentially the energy scale at which the effective theory breaks down. Thus, the interesting physics is normally given by the lowest possible order field operator as the higher are suppressed by powers of Λ.

2.2.1 Cross sections

Since the DM is non-relativistic, the energy transfer in interactions is small. If χ is a fermion, one can expand the fermion spinors in the non-relativistic limit as $u \to \sqrt{m}(\xi,\ \xi)^T$ and $v \to \sqrt{m}(\eta,\ -\eta)^T$. In the non-relativistic limit, the dimension 6 operators that are found by integrating out real scalars and vector bosons can then be written:

$$\mathcal{L}_S = \sum_q \frac{C_S^q}{\Lambda^2} \bar{\chi}\chi\bar{q}q,$$

$$\mathcal{L}_V = \sum_q \frac{C_V^q}{\Lambda^2} \bar{\chi}\gamma^\mu\chi\bar{q}\gamma_\mu q,$$

$$\mathcal{L}_A = \sum_q \frac{C_A^q}{\Lambda^2} \bar{\chi}\gamma^\mu\gamma^5\chi\bar{q}\gamma_\mu\gamma^5 q$$

where the sum is over all quarks and C_S^q, C_V^q and C_A^q are coupling constants. By integrating out pseudoscalars, complex scalars and particles that interact with gluons, the number of possible dimension 6 operators is larger but irrelevant as they can be shown to be proportional to the operators above in the non-relativistic limit (see e.g. ref. [60]). When expanding the spinors of the fermion fields, one also

find that the operators $\mathcal{L}_S$ and $\mathcal{L}_V$ yields spin independent cross sections while $\mathcal{L}_A$ yield spin dependent cross sections.

The cross section is conventionally expressed in terms of the zero momentum transfer cross section and a form factor [25]:

$$\frac{d\sigma}{d|\mathbf{q}|^2} = \frac{\sigma_0}{4m_r^2 v^2} F(|\mathbf{q}|). \tag{2.2}$$

In the equation above, m_r is the reduced mass and v is the relative velocity. $F(|\mathbf{q}|)$ is a form factor, which is normalized such that $F(0) = 1$. The total zero momentum cross section σ_0 is defined as

$$\sigma_0 = \int_0^{4m_r^2 v^2} \frac{d\sigma(q=0)}{d|\mathbf{q}|^2} d|\mathbf{q}|^2. \tag{2.3}$$

The momentum dependence of the actual cross section is thus described entirely by the form factor.

The spin independent and spin dependent zero momentum cross sections σ_0^{SI} and σ_0^{SD} corresponding to the operators discussed above can be written [59]:

$$\sigma_0^{SI} = \frac{m_r^2}{\pi \Lambda^4} \left[Z f_p + (A - Z) f_n \right]^2, \tag{2.4}$$

$$\sigma_0^{SD} = \frac{4m_r^2}{\pi \Lambda^4} \left[\sum_{q=u,d,s} d_q \lambda_q \right]^2 J_N (J_N + 1). \tag{2.5}$$

For $\mathcal{L}_S$, the factors f_p and f_n are calculated from chiral perturbation theory [61–63]. For $\mathcal{L}_V$, $f_p = 2b_u + b_d$ and $f_n = b_u + 2b_d$ where b_u and b_d are the coupling constants to the up and down quarks. For the spin dependent cross sections, J_N is the spin of the nucleus, d_q the the coupling constant to quark q and λ_q is given by

$$\lambda_q = \frac{\langle S_p \rangle}{J_N} \Delta_q^p + \frac{\langle S_n \rangle}{J_N} \Delta_q^n \tag{2.6}$$

where $\langle S_{p,n} \rangle / J_N$ is the fraction of spin carried by the protons and neutrons and Δ_q^n is the part of the spin carried by quark q in nucleon n.

Chapter 3

Solar capture of dark matter

3.1 Capture of dark matter

The first calculation of the capture rate was done by Press and Spergel [64]. Gould improved their results and corrected a few errors in his first paper [65] and compactified the calculations greatly in a second [66]. The following derivation is that of Goulds first paper. Consider a spherical shell in a spherically symmetric gravitational field centered at $\boldsymbol{r} = 0$. The radius of the shell is r with thickness dr and escape velocity $v_{\rm esc}(r) = v$, the DM velocity distributions $f_\chi(u)$ and $f_{\bar{\chi}}(u)$ are defined such that $\int f(u)du$ yield the local DM number density n_χ and $n_{\bar{\chi}}$ respectively. At a point R where the gravitational field is negligible, the DM flux through an infinitesimal area element is

$$dF = \frac{1}{4} u f(u)\, du\, d\cos^2\theta\ ,\ \ 0 < \theta < \frac{\pi}{2}, \tag{3.1}$$

where θ is defined relative to the radial direction. Changing variables $J = Ru\sin\theta$ and multiplying by the area of the shell yield the total number of particles entering the shell with velocity u.

$$dN = \pi \frac{f(u)}{u}\, du\, dJ^2\ ,\ \ 0 < J^2 < r^2 w^2 \tag{3.2}$$

At radius r, the velocity of particles is given by $w^2 = u^2 + v^2$ due to conservation of energy. The probability of DM capture by scattering in the shell can be written as

$$P_{\rm cap} = \Omega(r, w)\frac{dl}{w}, \tag{3.3}$$

where $\Omega(r, w)$ is related to the probability per second to scatter to a velocity less than v and dl/w is the time spent in the shell which is easily calculated to

$$\frac{dl}{w} = \frac{1}{w} \frac{2dr}{\sqrt{1 - (\frac{J}{rw})^2}} \theta(rw - J). \tag{3.4}$$

The heaviside function and the 2 take into account that particles cross the shell twice or not at all. dr/w times the radical is the time spent in the shell. The number of DM particles that are captured are dN times P_{cap}. Performing the integral over J^2 can also be done which results in the formula for capture

$$dC = 4\pi r^2 \frac{f(u)}{u} w\Omega(r, w)\, dr\, du. \tag{3.5}$$

By integrating over the radius of the body and over the velocity distribution, one find the total captured number of particles per second.

3.1.1 Solar element capture of dark matter

As there are many elements in the Sun, let us decompose the formula into the capture of DM onto element i and sum over all elements, it is then given by

$$dC = \sum_i dC_i = \sum_i 4\pi r^2 \frac{f(u)}{u} w\Omega_i(r, w)\, du\, dr. \tag{3.6}$$

The total scattering rate is given by

$$\Omega_i(r, w) = \sigma_i(\Delta E) n_i(r) w P, \tag{3.7}$$

where ΔE is the energy loss of the DM particle, $n_i(r)$ is the density of element i and P is the probability of scattering to a velocity lower than the escape velocity. In a collision, the energy loss is uniformly distributed over an interval

$$0 < \frac{\Delta E}{E} < \frac{\mu}{\mu_+^2} \tag{3.8}$$

where $\mu = \frac{m_\chi}{M_i}$ and $\mu_+ = \frac{1+\mu}{2}$. For capture of a DM particle, the energy loss must be big enough to put its velocity below the escape velocity, i.e.,

$$\frac{\Delta E}{E} > \frac{w^2 - v^2}{w^2} = \frac{u^2}{w^2}. \tag{3.9}$$

The energy dependence of the nucleus-DM scattering cross section is more important for heavier elements than for hydrogen. The cross section is parametrized as

$\sigma = \sigma_i |F(q)|$, where σ_i is the nuclei-DM spin independent cross section at zero energy transfer. The probability to lose an energy ΔE in the collision, using Gould's form factor, is

$$P = \frac{\mu_+^2}{\mu} e^{-\Delta E/E_0} \tag{3.10}$$

where $E_0 = \frac{3\hbar^2}{2M_i R_i^2}$ and $R_i = [0.91(\frac{M_i}{\mathrm{GeV}})^{\frac{1}{3}} + 0.3] \cdot 10^{-15}\ m$. The total less-than-$v$ scatter rate is then

$$\Omega_i(r,w) = \sigma_i n_i(r) w \int_{\frac{u^2}{w^2}}^{\frac{\mu}{\mu_+^2}} \frac{\mu_+^2}{\mu} e^{-\Delta E/E_0} d\left(\frac{\Delta E}{\frac{1}{2}m_\chi w^2}\right) \theta\left(\frac{\mu}{\mu_+^2} - \frac{u^2}{w^2}\right). \tag{3.11}$$

The factor $w\Omega_i(r,w)$ can then be calculated to be

$$w\Omega_i(r,w) = \sigma_i n_i(r) \frac{2E_0}{m_\chi} \frac{\mu_+^2}{\mu} \left[e^{-\frac{m_\chi u^2}{2E_0}} - e^{-\frac{\mu}{\mu_+^2}\frac{m_\chi w^2}{2E_0}} \right] \theta\left(\frac{\mu}{\mu_+^2} - \frac{u^2}{w^2}\right). \tag{3.12}$$

For element i, if one assume that DM-proton and DM-neutron cross sections are approximately equal, σ_i can be related to the hydrogen spin independent cross section σ_H by

$$\frac{\sigma_i}{\sigma_H} = A_i^2 \frac{(m_\chi m_i)^2}{(m_\chi + m_i)^2} \frac{(m_\chi + m_H)^2}{(m_\chi m_H)^2}. \tag{3.13}$$

Here, A_i is the number of nucleons in the nuclei. For hydrogen we have

$$w\Omega_i(r,w) = \sigma_p n_H(r)(w^2 - \frac{\mu_+^2}{\mu}u^2)\theta\left(\frac{\mu}{\mu_+^2} - \frac{u^2}{w^2}\right) \tag{3.14}$$

where σ_p is the total DM-hydrogen spin dependent plus spin independent cross sections $\sigma_H^{SD} + \sigma_H$. The spin dependent cross sections onto nuclei larger than hydrogen is safely neglected. This is due to the low solar abundance of such elements, the form factor weakening, and lack of A^2 enhancement. The total capture rate is thus

$$C = \int_0^{R_\odot} 4\pi r^2 \int_0^\infty \sum_i \frac{f(u)}{u} w\Omega_i(r,w)\, du\, dr. \tag{3.15}$$

with $w\Omega_i(r,w)$ given in eqs. (3.12) and (3.14).

3.1.2 Dark matter self-capture

The self-capture of DM follow the same procedure as that of solar nuclei capture. For DM self-capture, the factor $\Omega(r, w)$ can be written as

$$\Omega_i(r, w) = \sigma_{\chi\chi} n(r) w P. \tag{3.16}$$

The factor P is the combined probability that the DM particle scatter to a velocity less than v while still not giving the target particle a velocity larger than v, since it would then escape and the change of trapped DM particles is zero. The energy transfer must then be inside the interval

$$\frac{u^2}{w^2} < \frac{\Delta E}{E} < \frac{v^2}{w^2}. \tag{3.17}$$

Since the transfer energy distribution is uniform,

$$w\Omega(r, w) = \sigma_{\chi\chi} n(r)(v^2 - u^2)\theta(v - u). \tag{3.18}$$

The captured DM particles are assumed to fall into thermal equilibrium with their surroundings quickly. The number density $n(r)$ will have the form

$$n(r) = n_0 e^{-m_\chi \phi(r)/kT}, \tag{3.19}$$

where $\phi(r)$ is the potential energy of a DM particle at a distance r from the center. Under the assumption that the DM distribution is concentrated inside a radius where the temperature T and density ρ is constant and equal to the core temperature T_c and core density ρ_c, then

$$\phi(r) = \frac{2\pi G \rho_c}{3} r^2 \tag{3.20}$$

and $n(r)$ can be written

$$n(r) = n_0 e^{-r^2/r_\chi^2} \tag{3.21}$$

where $r_\chi^2 = \frac{3kT_c}{2\pi G \rho_c m_\chi}$ and $n_0 = \pi^{-\frac{3}{2}} r_\chi^{-3} N$ since the integral of $n(r)$ over all space should yield the total number of trapped DM particles N. We define $\epsilon(r) = n(r)/N$. The self-capture rate is now given by

$$C_{\text{self}} = \int_0^{R_\odot} 4\pi r^2 \int_0^v \frac{f(u)}{u} \sigma_{\chi\chi} \epsilon(r)(v^2 - u^2) N \, du \, dr. \tag{3.22}$$

The same formula can be used to calculate the capture of DM on anti-DM by substituting $\sigma_{\chi\chi} \to \sigma_{\chi\bar{\chi}}$ and $N \to \bar{N}$.

When a DM particle hits a trapped anti-DM particle, the energy transferred may be high enough to eject the anti-DM particle resulting in a gain of a DM

and the loss of an anti-DM particle and thus result in a reducing correction to the self-capture constant. This occur when the energy transfer is in the interval

$$\frac{v^2}{w^2} < \frac{\Delta E}{E} < 1, \tag{3.23}$$

where 1 is the reduction of the factor μ/μ_+^2 when the masses of the projectile and target particles are the same. Again, the energy transfer is uniform and one finds that

$$w\Omega(r,w) = \sigma_{\chi\bar{\chi}} n(r) u^2 \theta(u). \tag{3.24}$$

The ejection rate of captured DM by anti-DM is given by

$$C_{\text{eject}} = \int_0^{R_\odot} 4\pi r^2 \int_0^\infty \frac{f(u)}{u} \sigma_{\chi\bar{\chi}} \epsilon(r) u^2 N \, du \, dr. \tag{3.25}$$

By substituting $N \to \bar{N}$, the ejection rate of anti-DM by DM can be calculated.

3.1.3 Annihilation of dark matter

The annihilation rate is given by [67]

$$\Gamma_A = \langle \sigma v \rangle \int_0^{R_\odot} 4\pi r^2 n(r) \bar{n}(r) \, dr, \tag{3.26}$$

where $\langle \sigma v \rangle$ is the thermally averaged cross section. Here, $n(r)$ and $\bar{n}(r)$ are the DM and anti-DM distribution functions. Assuming they are in thermal equilibrium as before, then

$$\Gamma_A = \langle \sigma v \rangle \int_0^{R_\odot} 4\pi r^2 e^{-2r^2/r_\chi^2} \frac{N\bar{N}}{\pi^3 r_\chi^6} \, dr. \tag{3.27}$$

Since the DM is located in the solar core, the number densities are negligible at large radii and the integral is very well approximated by integrating to infinity rather than $R_\odot$. Performing the integral gives the annihilation rate as

$$\Gamma_A = \langle \sigma v \rangle \frac{N\bar{N}}{(2\pi)^{3/2} r_\chi^3}. \tag{3.28}$$

Chapter 4

Time evolution of dark matter

Assuming that there are equal amounts of DM and anti-DM, the time evolution of the number of DM particles in the Sun is governed by the two equations;

$$\dot{N} = c + CN + \bar{C}\bar{N} - \Gamma N\bar{N}, \tag{4.1}$$

$$\dot{\bar{N}} = \bar{c} + \bar{C}N + C\bar{N} - \Gamma N\bar{N}. \tag{4.2}$$

c and $\bar{c}$ are the capture constants by solar nuclei, C and $\bar{C}$ are the self-capture constants, C_{self}/N and $C_{\text{self}}/\bar{N}$, and Γ is the annihilation constant $\Gamma_A/N\bar{N}$. The disregard for ejection will be left for the discussion in ch. 6. The solar nuclei capture constants are computed from eq. (3.15), the self-capture constants proportional to N and $\bar{N}$ with eq. (3.22) and Γ is calculated from (3.28). In principle, one should take into account the evaporation of DM particles from the Sun with a term $-C_E N$ on the right hand side of the equation for $\dot{N}$ and $-C_E\bar{N}$ in the equation for $\dot{\bar{N}}$. However, Gould showed that the evaporation of DM in the Sun is negligible for DM masses larger than roughly 3 GeV [68]. It is important to note that for large enough N and $\bar{N}$, the self-capture terms have an upper bound. Since we assume DM scatter only once, the effective cross section $\sigma_{\text{eff}} = \sigma_{\chi\chi}N + \sigma_{\chi\bar{\chi}}\bar{N}$ cannot increase beyond the surface of the DM distribution πr_χ^2.

For symmetric capture $c = \bar{c}$, which implies that $N = \bar{N}$, the system reduces to one equation:

$$\dot{N} = c + (C + \bar{C})N - \Gamma N^2. \tag{4.3}$$

Solving the equation above when $\dot{N} = 0$ will yield the equilibrium value for N and $\bar{N}$ when the total capture and annihilation rate are the same. This happens when

$$N = \frac{C + \bar{C}}{2\Gamma} + \frac{\sqrt{4c\Gamma + (C + \bar{C})^2}}{2\Gamma}. \tag{4.4}$$

The total amount of DM and anti-DM in the Sun is then two times this value.

4.1 Dark matter asymmetry

An asymmetry in the captured number of DM particles in the Sun can occur for two reasons. The capture rates of DM and anti-DM can be different due to different scattering cross sections on regular matter or there can be an asymmetry in the background density of DM and anti-DM (asymmetric dark matter) much like the asymmetry in the barynic sector. Even if the capture rates of DM and anti-DM is equal, the solar capture is a Poisson process and there will be some stochastic variations that can give rise to an asymmetry. The asymmetry Δ, is defined as $\Delta = N - \bar{N}$. By taking the difference between the equations for $\dot{N}$ and $\dot{\bar{N}}$, one obtain a differential equation in Δ which does not depend on the annihilation rate and can be solved analytically. Assuming that the DM is stable, the magnitude of Δ also represents the minimum amount of DM in the Sun.

$$\dot{\Delta} = c - \bar{c} + (C - \bar{C})\Delta = d + D\Delta. \tag{4.5}$$

The initial value of Δ at time $t = 0$ is taken to $\Delta(0) = 0$, assuming a negligible amount of DM and anti-DM in the Sun at its birth. By defining $\Delta = f \exp(Dt)$, the equation becomes

$$\dot{f} = de^{-Dt}\,, \qquad \Delta = \int_0^t de^{D(t-\tau)}\, d\tau. \tag{4.6}$$

4.1.1 Intrinsic different capture rates

If c and $\bar{c}$ are different, then $d \neq 0$. This can be from an asymmetry in the background DM or the cross sections for DM and anti-DM on solar nuclei are different. If we assume that c and $\bar{c}$ are constant in time we can write down a solution for Δ:

$$\Delta = \frac{d}{D}(e^{Dt} - 1). \tag{4.7}$$

There are three interesting limiting cases to this solution:

1. $|Dt| \ll 1$: There has not been enough for time for self-capture to increase the numbers of DM particles. Taylor expanding the exponential yield

   $$\Delta \simeq dt \tag{4.8}$$

   which is just the difference in collection rate of DM and anti-DM as expected if the self-capture is negligible.

2. $|Dt| \gg 1,\ D < 0$: The system has reached an equilibrium in which the DM captures the anti-DM more strongly than it captures itself. The asymptotic behaviour of Δ is

$$\Delta \to -\frac{d}{D}. \tag{4.9}$$

Δ reaches an equillibrium at the quote between the difference in solar nuclei and self-capture rates. The asymmetry caused by asymmetric capture on solar nucleons is balanced by DM more effectively capturing anti-DM.

3. $|Dt| \gg 1,\ D > 0$: DM capture itself more efficiently than it capture anti-DM.

$$\Delta \to \frac{d}{D} e^{Dt}. \tag{4.10}$$

The difference experiences an exponential growth. The overabundance of DM relative to anti-DM caused by asymmetric capture is enhanced by the self-capture.

4.1.2 Stochastically induced difference

If the capture rates for DM and anti-DM are equal, an asymmetry may still occur due to stochastic variations. Even if the variation decrease with time relative to the total number of captured particles, the captured DM is going to annihilate with anti-DM which may result in a significant asymmetry to be present in the long run. This can be modelled by assuming a white noise signal $\delta_c(t)$ on top of the regular capture rates for DM and anti-DM

$$c = c_0 + \delta_c(t), \quad \langle \delta_c(t) \rangle = 0, \quad \langle \delta_c(t)\delta_c(\tau) \rangle = s\delta(t-\tau). \tag{4.11}$$

The strength of the white noise signal is normalized so that the captured number n and its variation match those of a Poisson distribution, i.e., $\langle n^2 \rangle - \langle n \rangle^2 = \langle n \rangle$. Then

$$\begin{aligned} \langle n \rangle &= \left\langle \int_0^t c_0 + \delta_c(\tau)\, d\tau \right\rangle \\ &= c_0 t, \end{aligned} \tag{4.12}$$

$$\begin{aligned} \langle n^2 \rangle &= \left\langle \left(\int_0^t c_0 + \delta_c(\tau) d\tau \right)^2 \right\rangle \\ &= c_0^2 t^2 + 2c_0 t \int_0^t \langle \delta_c(\tau) \rangle d\tau + \int_0^t \int_0^t \langle \delta_c(\tau)\delta_c(\sigma) \rangle d\tau d\sigma \\ &= c_0^2 t^2 + st, \end{aligned} \tag{4.13}$$

and hence $s = c_0$. The same argument can be used for anti-DM with a white noise signal $\delta_{\bar{c}}(t)$ and we find

$$d = \delta_d(t) = \delta_c(t) - \delta_{\bar{c}}(t), \tag{4.14}$$

where δ_c and $\delta_{\bar{c}}$ are independent which give δ_d the following properties:

$$\langle \delta_d(t) \rangle = 0, \quad \langle \delta_d(t)\delta_d(s) \rangle = 2c_0\delta(t-s). \tag{4.15}$$

The expectation value of Δ is zero, which is fine since the likelihood that there is an overabundance of DM is the same as that of an equal overabundance of anti-DM. To estimate the typical magnitude of Δ, we can study $\tilde{\Delta} = \sqrt{\langle \Delta^2 \rangle}$. We find that

$$\begin{aligned} \tilde{\Delta}^2 &= \int_0^t \int_0^t e^{D(2t-\tau-\sigma)} \langle \delta_d(\tau)\delta_d(\sigma) \rangle d\tau d\sigma \\ &= 2c_0 \int_0^t e^{2D(t-\tau)} d\tau \\ &= \frac{c_0}{D}\left(e^{2Dt} - 1\right) \end{aligned} \tag{4.16}$$

The same limits as for the case of intrinsic asymmetry are of interest here:

1. $|Dt| \ll 1$: Negligible self-capture, an expansion of the right hand side yields

   $$\tilde{\Delta} \approx \sqrt{2c_0 t}, \tag{4.17}$$

   which is exactly what is expected from the difference of two Poisson distributions of expectation value $c_0 t$

2. $|Dt| \gg 1,\ D < 0$: DM captures anti-DM more efficiently. Any stochastically induced difference between DM and anti-DM is counteracted by self-capture. The asymptotic behaviour is now

   $$\tilde{\Delta} \to \sqrt{\frac{c_0}{-D}}. \tag{4.18}$$

   An equillibrium is reached where the self-capture is equal to the stochastically induced difference.

3. $|Dt| \gg 1,\ D > 0$: DM capture itself more efficiently than it capture anti-DM. The asymmetry in this limit is given by

   $$\tilde{\Delta} \to \sqrt{\frac{c_0}{D}} e^{Dt}. \tag{4.19}$$

   The stochastically induced difference is enhanced by the self-capture which now experience exponential growth.

Chapter 5

Capture and accumulated numbers

The calculations of the capture and annihilation rates are easily done with a MATLAB program, as is numerical solutions to the differential equations governing the time evolution of the number of captured DM and anti-DM particles. Here are defined various input parameters used in the MATLAB program that was written for these purposes followed by examples of calculations of capture rates and the DM and anti-DM numbers in the Sun.

5.1 Input parameters

5.1.1 Local density and velocity profile

Standard estimates of the local dark matter density give values around $\rho_{\rm DM} = 0.3\pm0.1$ GeV cm^{-3} [69]. Here, it is assumed that DM and anti-DM make up half of the local density, $\rho_\chi = \rho_{\bar{\chi}} = 0.15$ GeV cm^{-3}. The velocity distribution $f(u)$ of the DM halo is assumed to be a Maxwell-Boltzmann distribution that is shifted to the solar frame which moves through the halo at $v = 220$ km/s.

$$f_\chi(u) = n_\chi \sqrt{\frac{3}{2\pi}} \frac{u}{v\bar{v}} \left(e^{-\frac{3}{2}\frac{(u-v)^2}{\bar{v}^2}} - e^{-\frac{3}{2}\frac{(u+v)^2}{\bar{v}^2}} \right) \tag{5.1}$$

where $n_\chi = \rho_\chi/m_\chi$. $\bar{v}$ is the three dimensional velocity dispersion which for a Maxwell-Bolzmann distribution is given by $\sqrt{3/2}v_{\rm p} = 270$ km/s since the most probable velocity $v_{\rm p} = v$. The velocity distribution is identical for anti-DM.

5.1.2 Solar data

The particular data set used is the AGS05 model retrieved from [70]. The AGS05 model is adapted to the measured abundances of heavier elements in the solar photosphere in [71] which introduced the current mismatch between solar observations and theory. In this particular set, the radial distribution of all elements up to Ni is present. It also contains information on the temperature, pressure and mass distributions. The solar radius is $R_\odot = 6.9551 \cdot 10^8$ m, the solar mass $M_\odot = 1.9884 \cdot 10^{30}$ kg [15] and the age of the Sun of 4.57 billion years. The data is needed to compute the radial number density of elements and the escape velocity inside the Sun.

5.1.3 DM parameters

Limits on the spin independent and spin dependent cross sections of DM-solar elements were presented in section 2 and will be used when calculating the capture rates c and $\bar{c}$.

The self-interaction cross section bounds are usually given by the self-interaction cross section divided by the DM mass, σ/m_χ. By simulating the shape of galaxies and galaxy clusters with self-interacting DM models and match results to observations, several studies have put limits on the self-interaction of DM [72–77]. While a couple of these studies favor a self-interaction between 0.5 and 450 cm^2/g, the others set upper bounds below 1 cm^2/g, one as low as 0.02 cm^2/g. These studies thus present upper bounds but come in conflict for the lower ones.

The relic abundance of DM is has been very precisely derived from the WMAP and Planck experimental data. By solving the Boltzmann equation, the relic abundance relate to the thermally averaged annihilation cross section of DM. The calculation is rather standard and is performed in for example ref. [25]. Here, $\langle \sigma v \rangle$ is assumed velocity independent and taken to be $3 \cdot 10^{-26}$ cm^3/s.

5.2 Capture and annihilation

The MATLAB program calculates the capture rates on solar nuclei, c and $\bar{c}$, as well as the capture rates due to self-interactions on DM and anti-DM, C and $\bar{C}$. Since we are concerned with asymmetric capture, the only difference between the capture rates c and $\bar{c}$ and C and $\bar{C}$ is the cross section. The following examples are thus general for both capture of DM and anti-DM by solar nuclei and self-capture.

5.2.1 Solar capture

Figure 5.1 shows an example of the capture rates with a pure spin independent cross section and a pure spin dependent cross section of magnitude 1 fb as a function of mass using the parameters above. The capture rates on different elements depends on the mass of DM, heavier elements capture heavy DM particles more effectively

which is why the spin independent cross section capture falls off more slowly with mass than its spin dependent counter part. The bounds set on the cross sections allow for choices of spin dependent cross sections with which the capture rate is several orders of magnitude larger.

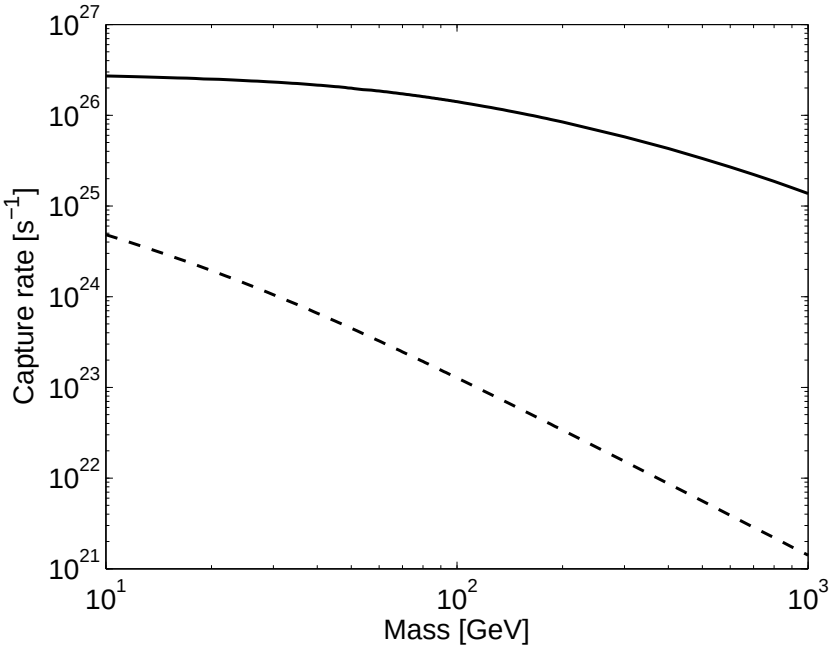

Figure 5.1. Capture rate as a function of DM mass for a spin independent DM-proton cross section (solid line) and a spin dependent cross section (dashed line), both at a magnitude of one fb.

5.2.2 Self-capture

The self-capture rate per trapped DM, C_{self}/N, is shown in figure 5.2. As can be seen, the capture rate falls off as m_χ^{-1}. Since heavy DM is expected to be concentrated to a very small volume in the core where the escape velocity is roughly constant. For masses less than a few GeV, the linearity is broken as the distribution of captured DM spreads into the outer regions of the Sun, where DM evaporation also becomes important. The ejection rate is, for $m_\chi = 5$ GeV and $\sigma_{\chi\chi} = \sigma_{\chi\bar{\chi}}$, about 2 orders of magnitude lower than the self-capture rate and becomes lower as the DM mass increases. Thus, for the ejection rate to be comparable to self-capture, $\sigma_{\chi\bar{\chi}} \gtrsim 10^2\, \sigma_{\chi\chi}$.

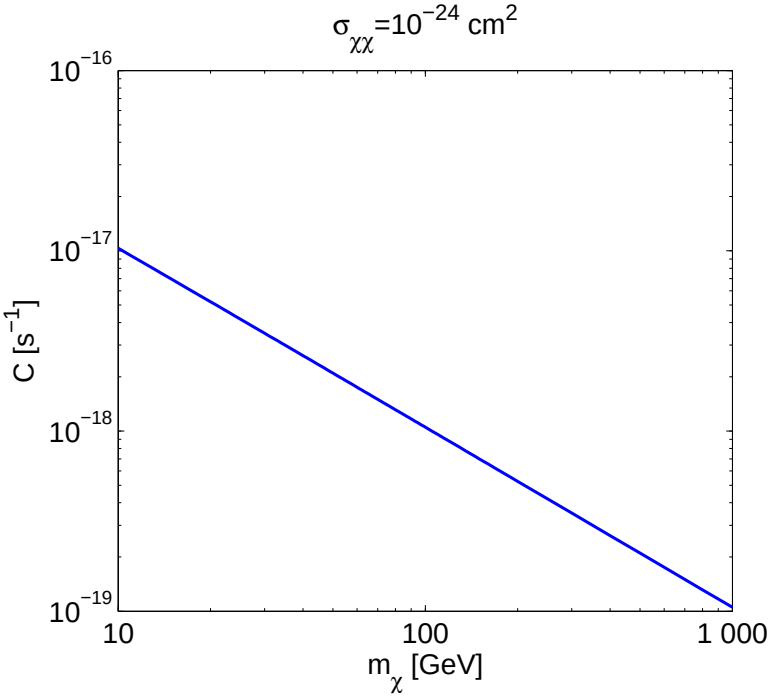

Figure 5.2. Self-capture constant as a function of mass and a DM-DM scattering cross section $\sigma_{\chi\chi}$ at 10^{-24} cm^2.

5.2.3 Annihilation

The annihilation constant as a function of mass is presented in figure 5.3. Γ increases as $m_\chi^{3/2}$. As in the case of self-capture, the annihilation rate is suppressed for small masses since the DM distributions spread out over a larger volume and the exponential dependence is broken as this occurs.

5.3 Accumulation of dark matter

It is apparent from the capture rates and annihilation constant that the number of DM and anti-DM particles in the Sun will be the highest for a low DM mass. The exponential behaviour of the asymmetry between DM and anti-DM for both the asymmetric case and stochastically induced case, Δ and $\tilde{\Delta}$ is apparent when $|Dt| \approx 1$. That is, $|D| > 6.9 \cdot 10^{-18}$ s^{-1} for $t = 4.57$ byrs. The most extreme cases for capture of DM occur for a spin dependent cross section of 10^{-37} cm^2 and a mass around 5 GeV at which the capture rate on nuclei is $c = 1.07 \cdot 10^{27}$ s^{-1} and so this is the largest capture rate allowed by experiments.

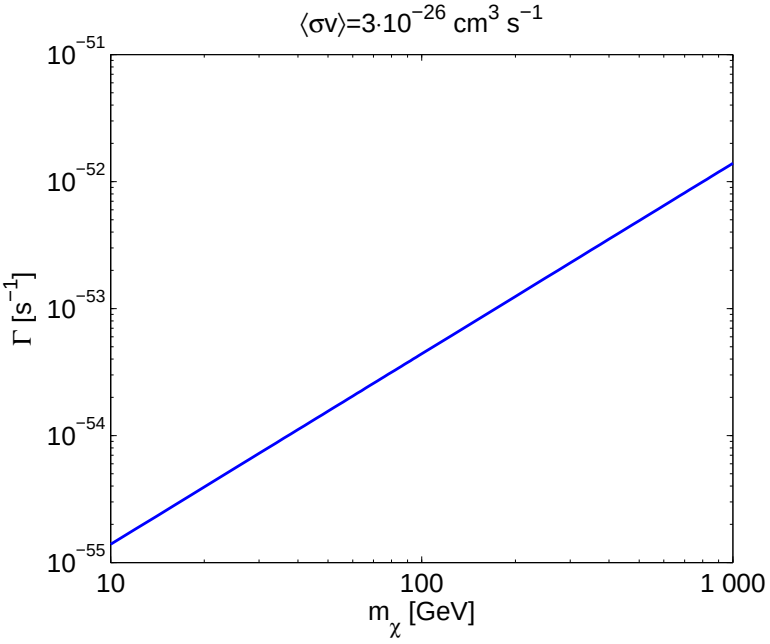

Figure 5.3. Annihilation constant as a function of mass using an annihilation cross section of $\langle \sigma v \rangle = 3 \cdot 10^{-26}$ cm^2

5.3.1 Symmetric capture and $\tilde{\Delta}$

The importance of self-capture is illustrated in figures 5.4 and 5.5. They show the sum of DM and anti-DM trapped in the Sun over time for two cases of capture rates. The value at which the number enters into equilibrium is given by eq. (4.3). It is apparent that this number is insensitive to self-capture when $4c\Gamma$ is larger than $(C + \bar{C})^2$. This can be seen in the first figure. The opposite case, when $(C + \bar{C})^2$ is larger than $4c\Gamma$, is shown in the second where the self-capture set the upper limit almost independently. It is apparent that the annihilation rate does not change much for self-capture when N depends mainly on c, but change drastically as the capture rate drops and self-interactions remain strong. For the case of figure 5.5, the annihilation rate is enhanced by a factor of almost 100. The limiting cases for the stochastically induced asymmetry are:

For very small self-interactions of DM, that is $|Dt| \ll 1$, $\tilde{\Delta}$ is given by $\sqrt{2ct}$, which evaluates to $1.76 \cdot 10^{22}$ for $c = 1.07 \cdot 10^{27}$ s^{-1} and t being the age of the Sun. Since heavier DM has a decreasing capture rate, $\tilde{\Delta}$ will never grow beyond this value for $|Dt| \ll 1$.

Figure 5.6 shows the evolution of $\tilde{\Delta}$ for various negative D. The magnitude of $\tilde{\Delta}$ increases with a large capture rate c and a small $|D|$. On the other hand, for the exponential to have kicked in, it is required that $|D| < 6.9 \cdot 10^{-18}$ s^{-1}. The

magnitude of $\tilde{\Delta}$ decreases with larger $|D|$ and is always smaller than the limit in which $|2Dt| \ll 1$ for the same c.

For the case of exponential growth, we have that $Dt \gg 1$. Figure 5.7 shows the growth of $\tilde{\Delta}$ over time for various D and $c = 10^{20}$ s^{-1}. For $D = 10^{-17}$ s^{-1}, the deviation from the case of small D is a factor of a few, while the exponential growth very pronounced for $D > 10^{-16}$ s^{-1}. For a D of $10^{-15.2}$ s^{-1}, the size of the asymmetry is roughly 10^{57} particles, at the same order of magnitude as the total number of atoms in the Sun. For the case of the largest c, the exponent of D change from -15.2 to -15.24 to reproduce the same asymmetry. The largest c requires the smallest D to give rise to such a large asymmetry and the difference $\sigma_{\chi\chi} - \sigma_{\chi\bar{\chi}}$ corresponding to this D is:

$$\frac{\sigma_{\chi\chi} - \sigma_{\chi\bar{\chi}}}{m_\chi} = 5.5{\cdot}10^{-24}\ \frac{\text{cm}^2}{\text{GeV}}. \tag{5.2}$$

Thus, for a given c smaller than 10^{27} s^{-1}, the difference $\sigma_{\chi\chi} - \sigma_{\chi\bar{\chi}}$ needs to be larger than the above. For the asymmetry to be 10 orders of magnitude smaller, $D = 10^{-15.33}$ s^{-1} which puts the difference in cross sections at

$$\frac{\sigma_{\chi\chi} - \sigma_{\chi\bar{\chi}}}{m_\chi} = 4.45{\cdot}10^{-24}\ \frac{\text{cm}^2}{\text{GeV}}. \tag{5.3}$$

5.3.2 Asymmetric capture and Δ

When the capture of DM and anti-DM is asymmetric, the asymptotic value of N and $\bar{N}$ can no longer be analytically determined whereas the difference Δ was analytically determined in equation 4.7. As for the case of stochastically induced asymmetries goes, the influence of self-capture on the value of Δ becomes important when $|Dt|$ is large. Unlike the stochastic case, Δ depend not on $\sqrt{c}$ but on d which in the maximal case is equal to c. For the case of asymmetric capture, the limiting cases are shown in figure 5.8 and 5.9. The first figure depicts the behaviour of Δ when D is negative and the second figure when D is positive.

In the limit $|Dt| \ll 1$, the largest asymmetry is when $d = c$ and c is maximal. At this point, for the age of the Sun, the asymmetry will be $1.44 \cdot 10^{44}$. If the Sun captures anti-DM, $\bar{c}$ will decrease d and the asymmetry will be smaller.

When D is negative and $|Dt| \gg 1$, Δ is maximised by a large d and a small D. For small enough D, the suppression of the exponential in Δ will still be strong and the asymmetry has not have had time to build up yet. The asymmetry due to small negative D will never exceed that of the case $|Dt| \ll 1$ for the same value of d.

When $Dt \gg 1$, the largest asymmetry occurs for $d = c$ and $c = 10^{27}$ s^{-1}. Figure 5.9 shows the asymmetry for this d and various D. The asymmetry is again

at the same order of magnitude as the total number of atoms in the Sun, 10^{57}, for a D of $10^{-15.6}$ s^{-1}. The corresponding difference in $\sigma_{\chi\chi} - \sigma_{\chi\bar{\chi}}$ is then

$$\frac{\sigma_{\chi\chi} - \sigma_{\chi\bar{\chi}}}{m_\chi} = 2.4{\cdot}10^{-24}\ \frac{\text{cm}^2}{\text{GeV}} \tag{5.4}$$

For an asymmetry 10 orders of magnitude lower, $D = 10^{-16.15}$ s^{-1} for which the difference in cross sections are

$$\frac{\sigma_{\chi\chi} - \sigma_{\chi\bar{\chi}}}{m_\chi} = 0.67{\cdot}10^{-24}\ \frac{\text{cm}^2}{\text{GeV}}. \tag{5.5}$$

For lower d, both cases require larger D than above in order to give rise to the same asymmetries.

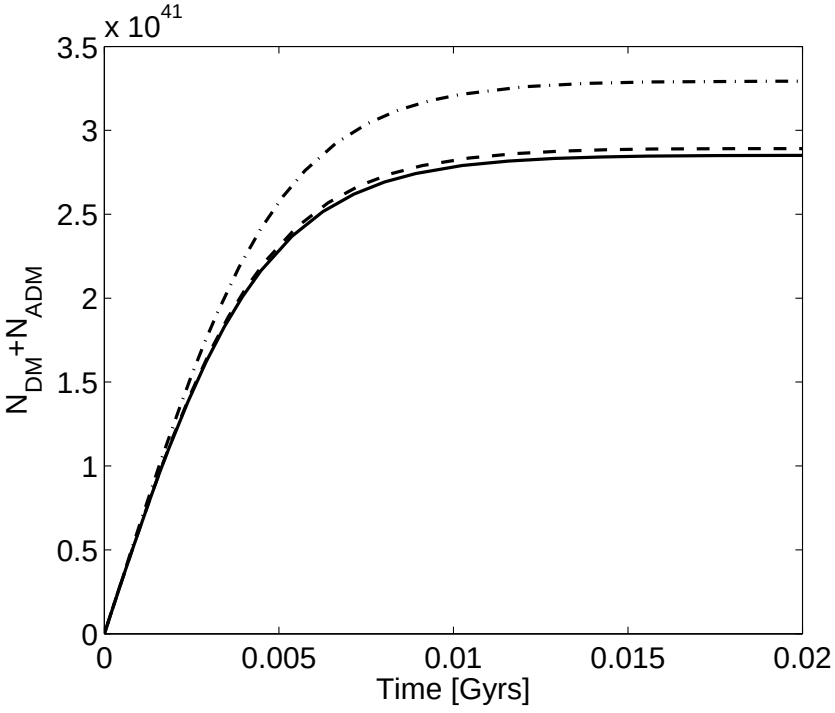

Figure 5.4. The sum of DM and anti-DM with $c = \bar{c} = 10^{27}$ s^{-1}, $\sigma_{\chi\bar{\chi}} = 0$ and mass $m_\chi = 5$ GeV. The lines correspond to different self-capture cross sections, solid: $\sigma_{\chi\chi} = 0$, dashed: $\sigma_{\chi\chi} = 10^{-23}$ cm^2, dash-dotted: $\sigma_{\chi\chi} = 10^{-22}$ cm^2.

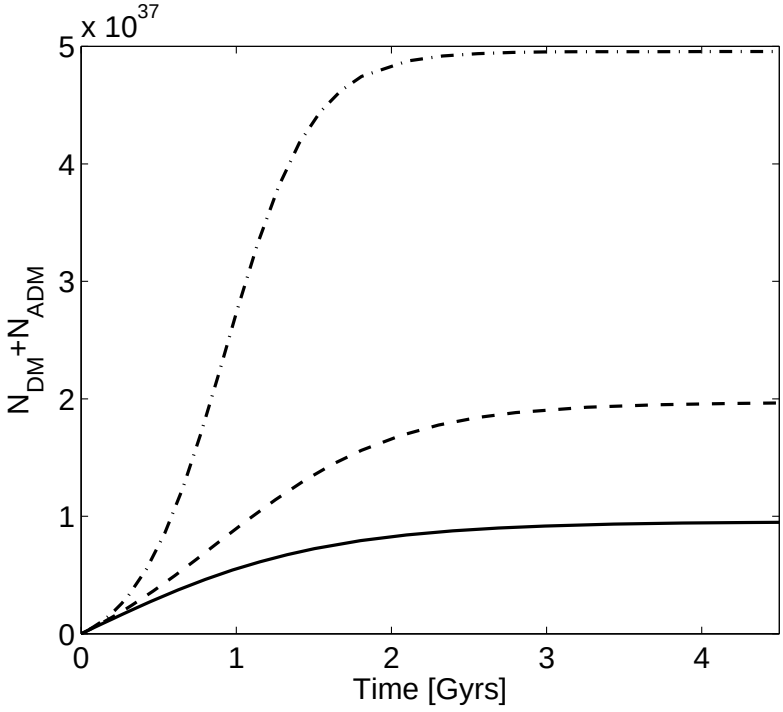

Figure 5.5. The sum of DM and anti-DM for $c = \bar{c} = 10^{20}$ s^{-1}, $\sigma_{\chi\bar{\chi}} = 0$ and mass $m_\chi = 100$ GeV. The lines correspond to different self-capture cross sections, solid: $\sigma_{\chi\chi} = 0$, dashed: $\sigma_{\chi\chi} = 10^{-22.5}$ cm^2, dash-dotted: $\sigma_{\chi\chi} = 10^{-22}$ cm^2.

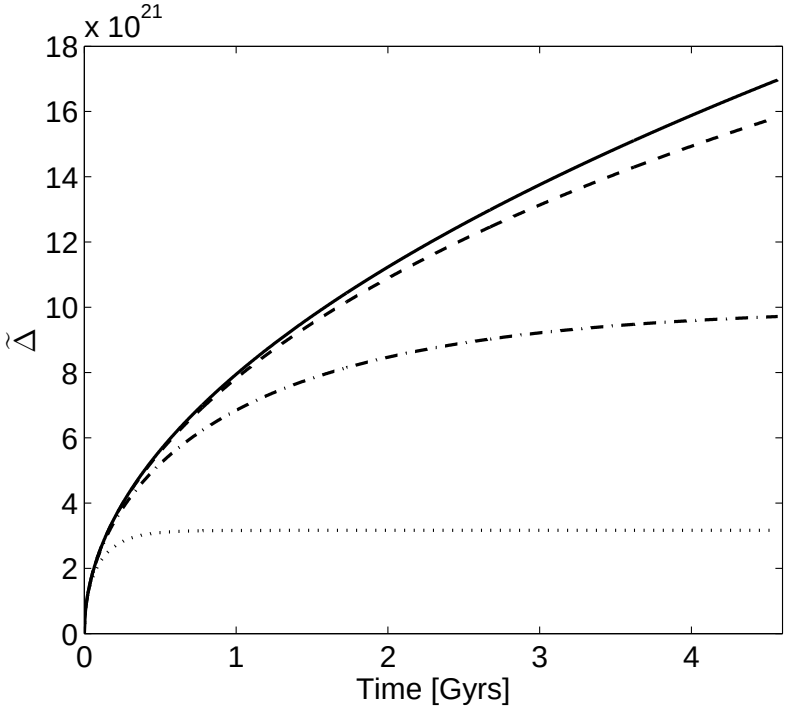

Figure 5.6. The stochastically induced asymmetry $\tilde{\Delta}$ over time with capture rates $c_0 = 10^{27}\ \mathrm{s}^{-1}$. The lines correspond to different negative D. solid: $D = -10^{-20}\ \mathrm{s}^{-1}$, dashed: $D = -10^{-18}\ \mathrm{s}^{-1}$, dash-dotted: $D = -10^{-17}\ \mathrm{s}^{-1}$, dotted: $D = -10^{-16}\ \mathrm{s}^{-1}$.

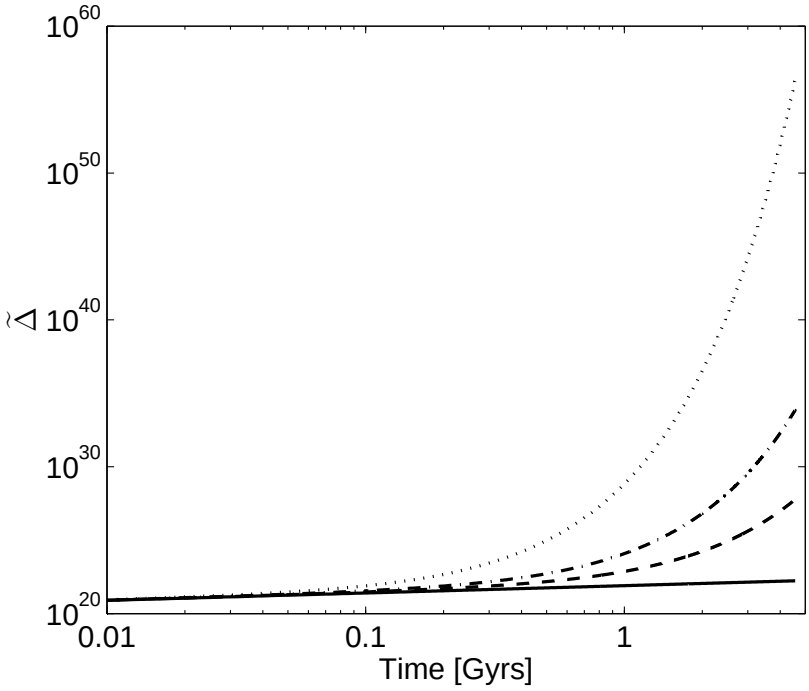

Figure 5.7. The stochastically induced asymmetry $\tilde{\Delta}$ over time with a capture rate $c_0 = 10^{27}$ s^{-1}. The lines correspond to different positive D; solid: $D = 10^{-20}$ s^{-1}, dashed: $D = 10^{-16}$ s^{-1}, dash-dotted: $D = 10^{-15.7}$ s^{-1}, dotted: $D = 10^{-15.25}$ s^{-1}.

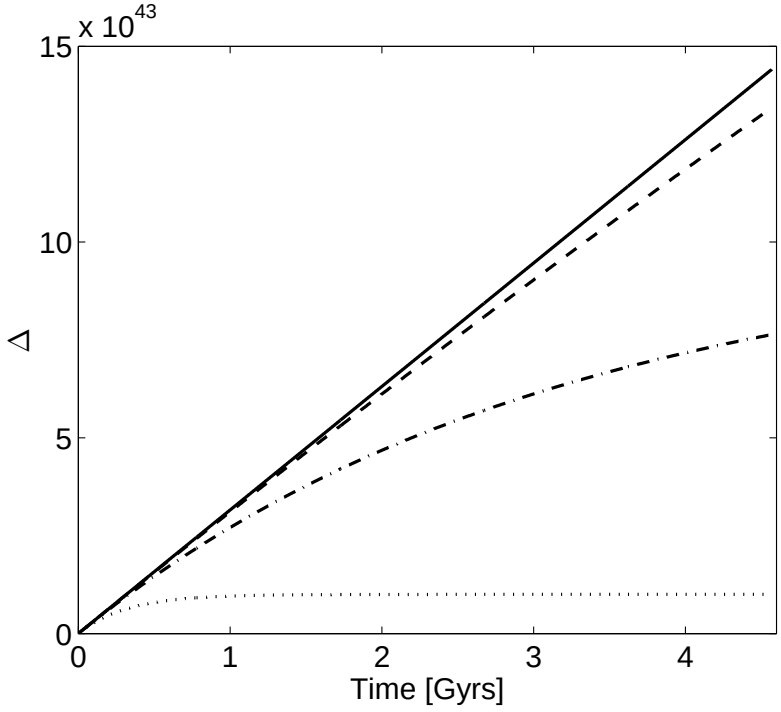

Figure 5.8. The asymmetry due to asymmetric capture Δ, using $d = 10^{27}$ s^{-1}. The lines correspond to different D; solid: $D = -10^{-20}$ s^{-1}, dashed: $D = -10^{-18}$ s^{-1}, dash-dotted: $D = -10^{-17}$ s^{-1}, dotted: $D = -10^{-16}$ s^{-1}.

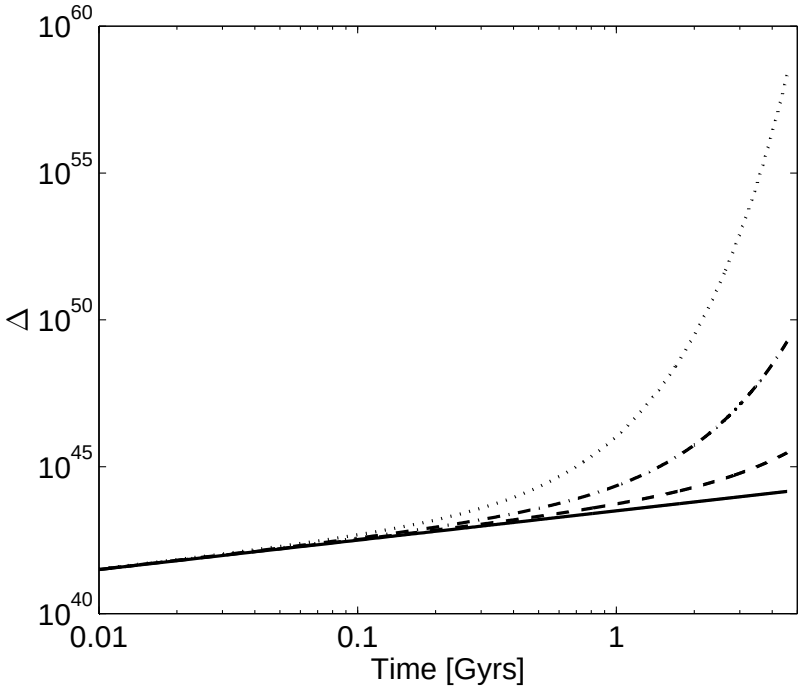

Figure 5.9. The asymmetry due to asymmetric capture Δ, using $d = 10^{27}$ s^{-1}. The lines correspond to different positive D with magnitudes; blue: $D = 10^{-20}$ s^{-1}, red: $D = 10^{-16.5}$ s^{-1}, magenta: $D = 10^{-16}$ s^{-1}, black: $D = 10^{-15.6}$ s^{-1}.

Chapter 6

Summary and conclusions

In this thesis, the accumulation of DM and anti-DM and the resulting asymmetries due to the stochastic nature of the capture process or asymmetric capture on solar nuclei was studied. The capture rates of DM, c, and anti-DM, $\bar{c}$, onto solar elements were calculated as well as the capture rates of DM, C, and anti-DM, $\bar{C}$, onto already captured DM and anti-DM particles as well as the annihilation rate. These parameters are necessary for the two equations governing the time evolution of the captured numbers. The difference between these two equations define the asymmetry. The asymmetry in the case of different capture rates of DM and anti-DM was found to be

$$\Delta = \frac{d}{D}(e^{Dt} - 1) \tag{6.1}$$

and for the stochastically induced asymmetry

$$\tilde{\Delta}^2 = \frac{c_0}{D}\left(e^{2Dt} - 1\right). \tag{6.2}$$

where $d = c - \bar{c}$, and $D = C - \bar{C}$ and c_0 is the common capture rate for when the capture is symmetric. For large capture rates, d needs to be many orders of magnitude smaller for $\tilde{\Delta}$ to be comparable in size. The largest allowed capture rate c, taking into account the limits on spin dependent and spin independent cross sections, is found to be about 10^{27} s^{-1}.

In the case of maximally asymmetric capture, $d = 10^{27}$ s^{-1}, to have an asymmetry of the same size as the number of particles in the Sun, $N_\odot = 10^{57}$, the difference in self-scattering cross sections was found to be:

$$\frac{\sigma_{\chi\chi} - \sigma_{\chi\bar{\chi}}}{m_\chi} = 2.4{\cdot}10^{-24}\ \frac{\text{cm}^2}{\text{GeV}}. \tag{6.3}$$

For $\Delta/N_\odot = 10^{-10}$, the interval is

$$\frac{\sigma_{\chi\chi} - \sigma_{\chi\bar{\chi}}}{m_\chi} = 0.67{\cdot}10^{-24}\ \frac{\text{cm}^2}{\text{GeV}}. \tag{6.4}$$

For smaller d, D is required to be larger to make up the asymmetry of said size.

For the stochastically induced asymmetry $\tilde{\Delta}$ using $c_0 = 10^{27}$ s^{-1}, the difference in self-scattering cross sections for $\tilde{\Delta} = N_\odot$ is

$$\frac{\sigma_{\chi\chi} - \sigma_{\chi\bar{\chi}}}{m_\chi} = 5.5{\cdot}10^{-24}\ \frac{\text{cm}^2}{\text{GeV}}, \tag{6.5}$$

and for $\tilde{\Delta}/N_\odot = 10^{-10}$

$$\frac{\sigma_{\chi\chi} - \sigma_{\chi\bar{\chi}}}{m_\chi} = 4.45{\cdot}10^{-24}\ \frac{\text{cm}^2}{\text{GeV}}, \tag{6.6}$$

For any c_0 smaller than the one used above increase the required difference in self-scattering cross sections. Unless $\sigma_{\chi\bar{\chi}}$ is much smaller than $\sigma_{\chi\chi}$, most of this range is ruled out by all studies but two. The relative size of the asymmetry to the number of atoms in the Sun are chosen with regard to the articles discussed in the effects on solar physics of DM. When D is negative or small, the relative number is not big enough to reach these numbers. The ejection of DM and anti-DM by scattering off other DM and anti-DM particles will decrease the value of D and will make up a sizeable correction when $\sigma_{\chi\bar{\chi}} \gtrsim \sigma_{\chi\chi}$. Only for the cases of small D and negative D will the ejection be important for the asymmetry in that the asymmetry will decrease and be less interesting with regard to effects on the Sun and thus, the ejection is neglected.

It is hard to draw conclusions on the asymmetric capture DM model even if the number of DM and anti-DM particles are high based on the asymmetric DM models due to heat injection in the core by annihilations of DM and anti-DM which do not occur when there is no captured anti-DM. A study on the effects of DM using the asymmetric capture model is necessary to draw conclusions.

Bibliography

[1] J. Thompson, *Cathode Rays*, Phil. Mag. **44**, 293 (1897).

[2] J. Chadwick, *Possible Existence of a Neutron*, Nature **129**, 312 (1932).

[3] M. Gell-Mann, *A schematic model of baryons and mesons*, Phys. Lett. **8**, 214 (1964).

[4] G. Zweig, *An SU_3 model for strong interaction symmetry and its breaking*, CERN report No.8182/TH-401 (1964).

[5] P. W. Higgs, *Broken Symmetries and the Masses of Gauge Bosons*, Phys. Rev. Lett. **13**, 508 (1964).

[6] F. Englert and R. Brout, *Broken Symmetry and the Mass of Gauge Vector Mesons*, Phys. Rev. Lett. **13**, 321 (1964).

[7] G. S. Guralnik, C. R. Hagen and T. W. B. Kibble, *Global Conservation Laws and Massless Particles*, Phys. Rev. Lett. **13**, 321 (1964).

[8] ATLAS Collaboration, G. Aad *et al.*, *Observation of a new particle in the search for the Standard Model Higgs boson with the ATLAS detector at the LHC*, Phys. Lett. B **716**, 1 (2012), `arXiv:1207.7214`.

[9] CMS Collaboration, S. Chatrchyan *et al.*, *Observation of a new boson at a mass of 125 GeV with the CMS experiment at the LHC*, Phys. Lett. B **716**, 30 (2012), `arXiv:1207.7235`.

[10] Super-Kamiokande Collaboration, Y. Fukuda *et al.*, *Evidence for Oscillation of Atmospheric Neutrinos*, Phys. Rev. Lett. **81**, 1562 (1998), `hep-ex/9807003`.

[11] SNO Collaboration, Q. R. Ahmad *et al.*, *Direct Evidence for Neutrino Flavor Transformation from Neutral-Current Interactions in the Sudbury Neutrino Observatory*, Phys. Rev. Lett. **89** (2002), `nucl-ex/0204008`.

[12] KamLAND Collaboration, K. Eguchi *et al.*, *First Results from KamLAND: Evidence for Reactor Antineutrino Disappearance*, Phys. Rev. Lett. **90** (2003), `hep-ex/0212021`.

[13] RENO Collaboration, J. K. Ahn *et al.*, *Observation of Reactor Electron Antineutrinos Disappearance in the RENO Experiment*, Phys. Rev. Lett. **108** (2012), arXiv:1204.0626.

[14] Daya Bay Collaboration, F. P. An *et al.*, *Observation of Electron-Antineutrino Disappearance at Daya Bay*, Phys. Rev. Lett. **108** (2012), arXiv:1203.1669.

[15] Particle Data Group, J. Beringer *et al.*, *Review of Particle Physics*, Phys. Rev. D **86** (2012).

[16] F. Zwicky, *Die Rotverschiebung von extragalaktischen Nebeln*, Helv. Phys. Acta **6**, 110 (1933).

[17] H. W. Babcock, *The rotation of the Andromeda nebula*, Lick Observatory bulletin **19** (1939).

[18] D. Clowe, A. Gonzalez and M. Markevitch, *Weak-Lensing Mass Reconstruction of the Interacting Cluster 1E 0657-558: Direct Evidence for the Existence of Dark Matter*, Astrophys. J. **604**, 596 (2004).

[19] A. Mahdavi *et al.*, *A dark core in Abell 520*, Astrophys. J. **668**, 806 (2007).

[20] D. J. Fixsen *et al.*, *The Cosmic Microwave Background Spectrum from the Full COBE/FIRAS Data Set*, Astrophys. J. **473** (1996), astro-ph/9605054.

[21] WMAP Collaboration, C. L. Bennett *et al.*, *Nine-Year Wilkinson Microwave Anisotropy Probe (WMAP) Observations: Final Maps and Results*, (2012), arXiv:1212.5225.

[22] Planck Collaboration, P. A. R. Ade *et al.*, *Planck 2013 results. I. Overview of products and scientific results*, (2013), arXiv:1303.5062.

[23] M. Milgrom, *A modification of the Newtonian dynamics as a possible alternative to the hidden mass hypothesis*, Astrophys. J. **270**, 365 (1983).

[24] J. Moffat, *A new nonsymmetric gravitational theory*, Phys. Lett. B **355**, 447 (1995), gr-qc/9411006.

[25] G. Jungman, M. Kamionkowski and K. Griest, *Supersymmetric dark matter*, Phys. Rep. **267**, 195 (1996).

[26] G. Bertone, D. Hooper and J. Silk, *Particle dark matter: evidence, candidates and constraints*, Phys. Rep **405**, 279 (2005), hep-ph/0404175.

[27] R. Bernabei *et al.*, *Particle dark matter signal in DAMA/LIBRA*, Nucl. Inst. and Meth. A **692**, 120 (2012).

[28] G. Angloher *et al.*, *Results from 730 kg days of the CRESST-II Dark Matter search*, Eur. Phys. J. C **72** (2011).

[29] CoGent Collaboration, C. Aalseth *et al.*, *Results from a Search for Light-Mass Dark Matter with a P-type Point Contact Germanium Detector*, Phys. Rev. Lett. **106** (2011), arXiv:1002.4703.

[30] CDMS Collaboration, R. Agnese *et al.*, *Dark Matter Search Results Using the Silicon Detectors of CDMS II*, (2013), arXiv:1304.4279.

[31] XENON100 Collaboration, E. Aprile *et al.*, *Dark Matter Results from 225 Live Days of XENON100 Data*, Phys. Rev. Lett. **109** (2012), arXiv:1207.5988.

[32] EDELWEISS Collaboration, E. Armengaud *et al.*, *A search for low-mass WIMPs with EDELWEISS-II heat-and-ionization detectors*, Phys. Rev. D **86** (2012), arXiv:1207.1815.

[33] S. Archambault *et al.*, *Dark matter spin-dependent limits for WIMP interactions on 19F by PICASSO*, Phys. Lett. B **682**, 185 (2009), arXiv:0907.0307.

[34] XENON Collaboration, E. Aprile *et al.*, *Limits on spin-dependent WIMP-nucleon cross sections from 225 live days of XENON100 data*, (2013), arXiv:1301.6620.

[35] Fermi LAT Collaboration, M. Ackermann *et al.*, *Measurement of Separate Cosmic-Ray Electron and Positron Spectra with the Fermi Large Area Telescope*, Phys. Rev. Lett. **108** (2012), arXiv:1109.0521.

[36] PAMELA Collaboration, O. Adriani *et al.*, *An anomalous positron abundance in cosmic rays with energies 1.5-100 GeV*, Nature **458**, 607 (2009), arXiv:0810.4995.

[37] AMS Collaboration, M. Aguilar *et al.*, *First Result from the Alpha Magnetic Spectrometer on the International Space Station: Precision Measurement of the Positron Fraction in Primary Cosmic Rays of 0.5-300 GeV*, Phys. Rev. Lett. **110** (2013).

[38] H. Yüksel, M. D. Kistler and T. Stanev, *TeV Gamma Rays from Geminga and the Origin of the GeV Positron Excess*, Phys. Rev. Lett. **103** (2009), arXiv:0810.2784.

[39] P. Blasi, *Origin of the Positron Excess in Cosmic Rays*, Phys. Rev. Lett. **103** (2009), arXiv:0903.2794.

[40] Fermi LAT Collaboration, M. Ackermann *et al.*, *Constraining Dark Matter Models from a Combined Analysis of Milky Way Satellites with the Fermi Large Area Telescope*, Phys. Rev. Lett. **107** (2011), arXiv:1108.3546.

[41] Fermi LAT Collaboration, M. Ackermann *et al.*, *Constraints on the galactic halo dark matter from Fermi-LAT diffuse measurements*, Astrophys. J. **761** (2012), arXiv:1205.6474.

[42] H.E.S.S. Collaboration, A. Abramowski *et al.*, *Search for Photon-Linelike Signatures from Dark Matter Annihilations with H.E.S.S.*, Phys. Rev. Lett. **110** (2013), arXiv:1301.1173.

[43] H.E.S.S. Collaboration, A. Abramowski *et al.*, *Search for a Dark Matter Annihilation Signal from the Galactic Center Halo with H.E.S.S.*, Phys. Rev. Lett. **106** (2011), arXiv:1103.3266.

[44] MAGIC Collaboration (and others), J. Aleksic *et al.*, *Searches for dark matter annihilation signatures in the Segue 1 satellite galaxy with the MAGIC-I telescope*, JCAP **1106** (2011), arXiv:1103.0477.

[45] ANTARES Collaboration, S. Adrian-Martinez *et al.*, *First Search for Dark Matter Annihilation in the Sun Using the ANTARES Neutrino Telescope*, (2013), arXiv:1302.6516.

[46] IceCube Collaboration, M. G. Aartsen *et al.*, *Search for dark matter annihilations in the sun with the 79-string IceCube detector*, Phys. Rev. Lett. **110** (2013), arXiv:1212.4097.

[47] Super-Kamiokande Collaboration, T. Tanaka *et al.*, *An Indirect Search for WIMPs in the Sun using 3109.6 days of upward-going muons in Super-Kamiokande*, Astrophys. J. **742** (2011), arXiv:1108.3384.

[48] V. Barger *et al.*, *High energy neutrinos from neutralino annihilations in the Sun*, Phys. Rev. D **76** (2007), arXiv:0708.1325.

[49] M. Blennow, J. Edsjö and T. Ohlsson, *Neutrinos from WIMP Annihilations Obtained Using a Full Three-Flavor Monte Carlo Approach*, Astrophys. J. **0801** (2008), arXiv:0709.3898.

[50] R. Lehnert and T. J. Weiler, *Neutrino flavor ratios as diagnostic of solar WIMP annihilation*, Phys. Rev. D **77** (2008), arXiv:0708.1035.

[51] D. Spergal and W. Press, *Effects of hypothetical, weakly interacting, massive particle on energy transport in the solar interior*, Astrophys. J. **294**, 663 (1985).

[52] M. Asplund, N. Grevesse and J. Sauval, *The solar chemical composition*, Nucl. Phys A **777** (2006), astro-ph/0410214.

[53] C. Pẽna-Garay and A. Serenelli, *Solar neutrinos and the solar composition problem*, (2008), arXiv:0811.2424.

[54] A. M. Serenelli *et al.*, *New solar composition: The problem with solar models revisited*, Astrophys. J. Lett. **705** (2009).

[55] M. T. Frandsen and S. Sarkar, *Asymmetric Dark Matter and the Sun*, Phys. Rev. Lett. **105** (2010), arXiv:1003.4505.

[56] D. T. Cumberbatch *et al.*, *Light WIMPs in the Sun: Constraints from Helioseismology*, Phys. Rev. D **82** (2010), arXiv:1005.5102.

[57] M. T. F. Iocco *et al.*, *Effect of low mass dark matter particles on the Sun*, (2010), arXiv:1005.5711.

[58] N. S. Kardashev, A. V. Tutukov and A. V. Fedorova, *Limits on the Mass of Dark Matter in the Sun from a Model for the Modern Sun and Its Previous Evolution*, Astron. Rep. **49**, 134 (2005).

[59] P. Agrawal *et al.*, *A Classification of Dark Matter Candidates with Primarily Spin-Dependent Interactions with Matter*, (2010), arXiv:1003.1912.

[60] K. Cheung *et al.*, *Global Constraints on Effective Dark Matter Interactions: Relic Density, Direct Detection, Indirect Detection, and Collider*, (2012), arXiv:1201.3402.

[61] T. P. Cheng, *Chiral symmetry and the Higgs-boson-nucleon coupling*, Phys. Rev. D **38**, 2869 (1988).

[62] H. Y. Cheng, *Low-energy interactions of scalar and pseudoscalar Higgs bosons with baryons*, Phys. Lett. B **219**, 347 (1989).

[63] J. Ellis, A. Ferstl and K. A. Olive, *Re-Evaluation of the Elastic Scattering of Supersymmetric Dark Matter*, Phys. Lett. B **481**, 304 (2000), hep-ph/0001005.

[64] W. H. Press and D. N. Spergel, *Capture by the sun of a galactic population of weakly interacting massive particles*, Astrophys. J. **296**, 679 (1985).

[65] A. Gould, *Resonant enhancements in WIMP capture by the earth*, Astrophys. J. **321**, 571 (1987).

[66] A. Gould, *Cosmological density of WIMPs from solar and terrestrial annihilations*, Astrophys. J. **388**, 338 (1992).

[67] K. Griest and D. Seckel, *Cosmic asymmetry, neutrinos and the sun*, Phys. Lett. B **283**, 681 (1987).

[68] A. Gould, *WIMP Distribution In And Evaporation From The Sun*, Astrophys. J. **321**, 560 (1987).

[69] J. Bovy and S. Tremaine, *On the local dark matter density*, Astrophys. J. **756**, 89 (2012), arXiv:1205.4033.

[70] Homepage of A. Serenelli, http://www.mpa-garching.mpg.de/~aldos/.

[71] M. Asplund, N. Grevesse and J. Sauval, *The solar chemical composition*, (2004), astro-ph/0410214.

[72] D. N. Spergel and P. J. Steinhardt, *Observational Evidence for Self-Interacting Cold Dark Matter*, Phys. Rev. Lett. **84**, 3760 (2000), astro-ph/9909386.

[73] N. Yoshida *et al.*, *Weakly Self-Interacting Dark Matter and the Structure of Dark Halos*, Astrophys. J. Lett. **544**, L87 (2000), astro-ph/0006134.

[74] R. Davè *et al.*, *Halo Properties in Cosmological Simulations of Self-Interacting Cold Dark Matter*, Astrophys. J. **547**, 574 (2001), astro-ph/0006218.

[75] O. Y. Gnedin and J. P. Ostriker, *Limits on Collisional Dark Matter from Elliptical Galaxies in Clusters*, Astrophys. J. **561**, 61 (2001), astro-ph/0010436.

[76] J. Miralda-Escudé, *A Test of the Collisional Dark Matter Hypothesis from Cluster Lensing*, Astrophys. J. **564**, 60 (2002), astro-ph/0002050.

[77] S. W. Randall *et al.*, *Constraints on the Self-Interaction Cross-Section of Dark Matter from Numerical Simulations of the Merging Galaxy Cluster 1E 0657-56*, Astrophys. J. **679**, 1173 (2008), arXiv:0704.0261.